

N 70 35595

CR 110012

A HIGH VOLTAGE, LOW CURRENT POWER
SOURCE FOR LONG TERM SPACE
APPLICATIONS

by

Michael L. Grygiel

NGK 22-009-019

CSR T-70-2

May 1970

CENTER FOR SPACE RESEARCH
MASSACHUSETTS INSTITUTE OF TECHNOLOGY



CASE FILE
COPY

A HIGH VOLTAGE, LOW CURRENT POWER
SOURCE FOR LONG TERM SPACE
APPLICATIONS

by

Michael L. Grygiel

NGH 22-009-019

CSR T-70-2

May 1970

A HIGH VOLTAGE, LOW CURRENT
POWER SOURCE FOR LONG TERM SPACE
APPLICATIONS

by

Michael L. Grygiel

S.B., United States Military Academy
(1968)

Submitted in Partial Fulfillment
of the Requirements for the
Degree of Master of Science
at the
MASSACHUSETTS INSTITUTE OF TECHNOLOGY

June 1970

Signature of Author _____

Department of Nuclear Engineering,
May 21, 1970

Certified by _____

Thesis Supervisor

Accepted by _____

Chairman, Departmental Committee
on Graduate Students

I would like to express my gratitude to my wife, Kathy, without whose cooperation and understanding this paper would not have been possible.

TABLE OF CONTENTS

Page	4	Chapter I, Introduction
Page	7	Chapter II, Statement of the Problem
Page	8	Chapter III, Previous Work
Page	10	Chapter IV, Theory
Page	21	Chapter V, The Experiment
Page	33	Chapter VI, Calculation and Results
Page	37	Chapter VII, Interpretation of the Results
Page	42	Chapter VIII, Conclusions
Page	44	Chapter IX, Specific Examples
Page	54	References

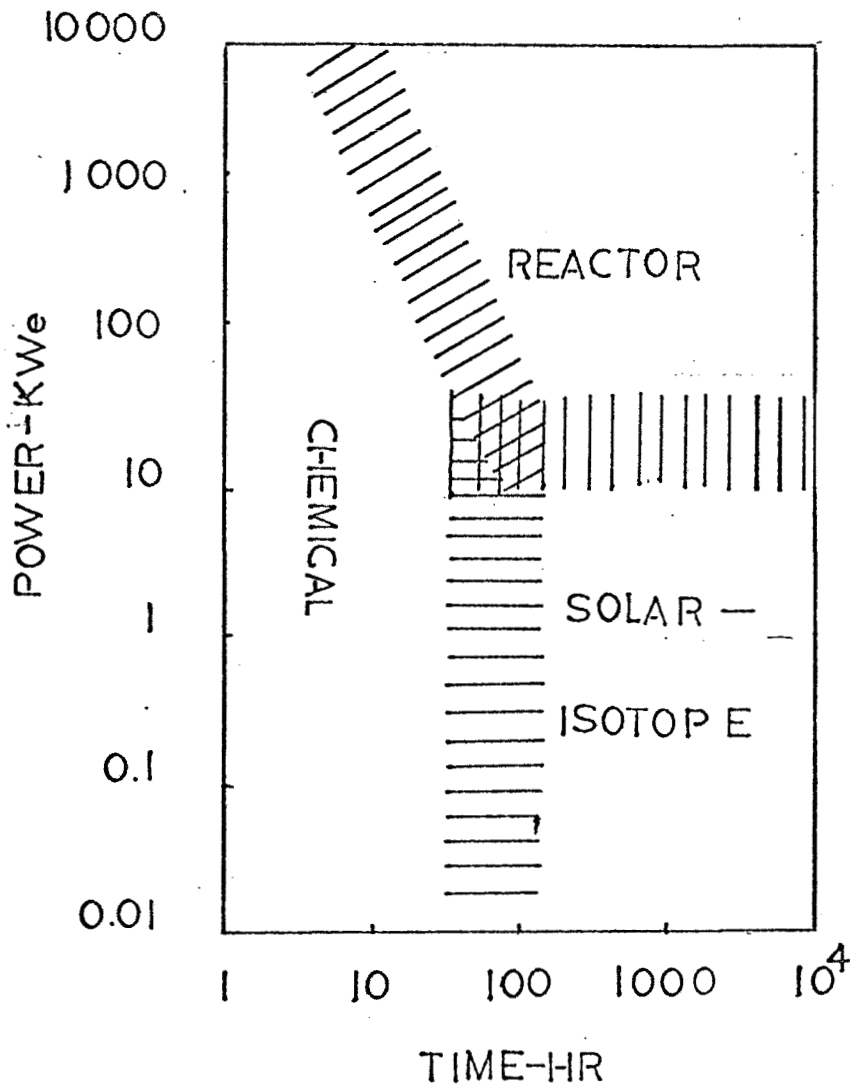
CHAPTER I
INTRODUCTION

Although man has recently acquired the ability to travel to the moon and will, in time, reach the other planets, the majority of space exploration in the next several years will be accomplished with unmanned vehicles. Because most of these missions will be to one or more of the planets, they will be of long duration.

To supply power requirements of these space vehicles long-lived, reliable power sources must be used. Because the varied power requirements will range from low voltage, high current to high voltage, low current drains, it will be necessary to provide several systems to supply the power. Figure 1 (4, Ch. 1) illustrates the capabilities of various power production methods. As can be seen, only reactors, solar cells and radioisotopes are suitable for long range missions. Because of their dependence on solar energy, solar cells would not be suitable for missions to the outer planets and must be eliminated.

This investigation concerns itself with using directly the energy from a radioactive source to produce high voltage, low current electricity. Such a device occupies the extreme lower right corner of Figure 1. It is clearly possible to produce the high current and low voltage requirements with reactors and radioisotopes in conjunction with mechanical cycles or thermionic or thermoelectric converters. (3,4)

FIG-1



POWER AND DURATION REGIONS FOR VARIOUS ENERGY SOURCES

The production of high voltages has previously been accomplished by the use of transformers or rotating machinery. For the production of 10 KV both of these methods involve complex and expensive equipment. A device for the direct conversion of nuclear energy to electrical energy seems to hold a great deal of promise as long as the current requirements do not exceed the microamp range. Such devices would be extremely simple and design and, therefore, very reliable and inexpensive. As with all radioisotopic power sources, their lifetimes would depend on the isotope employed. Radiation hazards could be designed to be quite low.

CHAPTER II

STATEMENT OF THE PROBLEM

It is the purpose of this investigation to produce a design of a high voltage, low current power source for use on an unmanned, long term space mission. The duration of the mission is estimated to be between three and five years. The design current and voltage requirements are in the vicinity of one microampere and 10 KV respectively. The weight of the device is to be as low as possible while maintaining the requirements of the source. Dose level outside the source is to be compatible with instrumentation aboard the vehicle. Because specific dose levels were not available at the time of this paper, dose levels will be reduced as much as is allowed by the other constraints of the problem.

The method of attack will be to design and build a device using laboratory amounts of activity and to test this device under simulated space conditions. Current and voltage measurements taken on this source will be extrapolated to obtain the characteristics of a prototype power source.

Due to the low quality vacuum employed in the experiment and the inexact construction of the device there will be some uncertainty in the results. Nevertheless, they should give a good feel for what might be expected from this type of source.

CHAPTER III
PREVIOUS WORK

Previous work in the field of obtaining high voltage and/or current from a radioactive material was done as early as 1913 by Mosley (11). Using silver spheres in a vacuum and twenty millicuries of radium he obtained a voltage of 150 KV immediately before breakdown. The current produced was calculated to be about 10^{-11} amps. The next significant work done in the field was by E.G. Linder and S.M. Christian at RCA in Princeton, New Jersey (7, 8, 9). Their source material was 250 millicuries of $\text{Sr}^{90}\text{-Y}^{90}$. The geometry was essentially cylindrical. The $\text{Sr}^{90}\text{-Y}^{90}$ was contained on the inner surface of a nickel cylinder and placed in an evacuated copper collector cylinder plated with aluminum. Results obtained from this apparatus were 1.05×10^{-9} amps at zero voltage and a peak voltage of 365 KV.

In the early fifties, J.H. Coleman (2) experimented with a solid insulating material separating his electrodes instead of a vacuum. The geometry was again cylindrical and the components were made of aluminum. Using 25 millicuries of $\text{Sr}^{90}\text{-Y}^{90}$, a zero voltage current of 5×10^{-11} amps was obtained. 3×10^{-10} amps were available at 100% collection efficiency. Using 10 millicuries 4×10^{-11} amps were obtained

out of 1.2×10^{-10} amps available. A maximum voltage of 7000 V was reached. No appreciable change in current was reported as the voltage increased.

In all cases, the conclusions drawn were that the sources worked well, but the amount of power they produced was so small it could not be used. Application of material with high concentrations of radioactive nuclei obtained from reactor cases (1) was evidently not considered. In the investigation it is hoped to extend the results outlined above by designing a one μ amp power supply employing the highly concentrated materials mentioned above.

CHAPTER IV

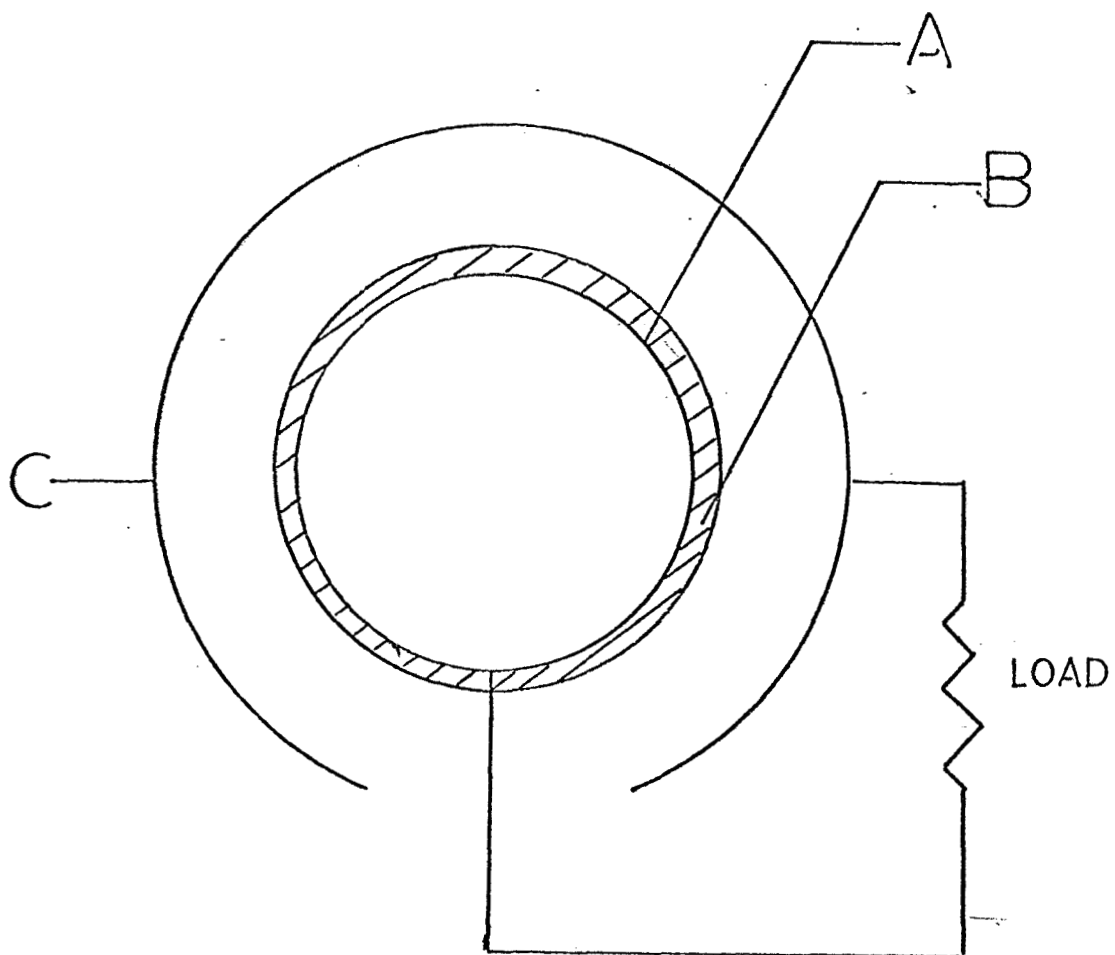
THEORY

The basic configuration of the power source is shown in Figure 2. A layer of radioactive material (B) is coated on a hollow conducting support sphere (A). A hollow conducting collector sphere (C) is electrically insulated from the support sphere which it surrounds.

Either an α or a β^- emitting material may be used to coat the support sphere. If a β^- source were used, the β^- particles leaving the support sphere would leave a net positive charge there. The β^- particles would strike the collector sphere, which would be thick enough to stop all of them, and leave a net negative charge on it. The accumulated charge would result in a potential being created across the gap between the two spheres. As a result of this potential, a current would flow from the support sphere through the load to the collector. If an α source were substituted for the β^- source, the charges would be reversed.

The voltage is limited by the separation of the two spheres (10). This would be a poor method of voltage control, however, since a breakdown would result in a step voltage decrease and some time would be required for the voltage to recover. For reasons which will be explained

FIG-2

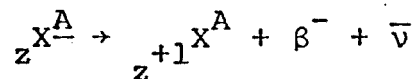


CROSS SECTION OF SPHERICAL POWER SOURCE

later, the current produced by the power source is almost constant with respect to changes in voltage. Because of this fact, the voltage can be controlled by regulating the resistance through which the current must flow.

Because this paper deals only with devices using β^- emitting source materials, the particular theory discussed will deal with this case. α emitting sources are not considered a good solution to the problem because the range of an α particle is so short that coating any amount of activity on a support sphere becomes a problem.

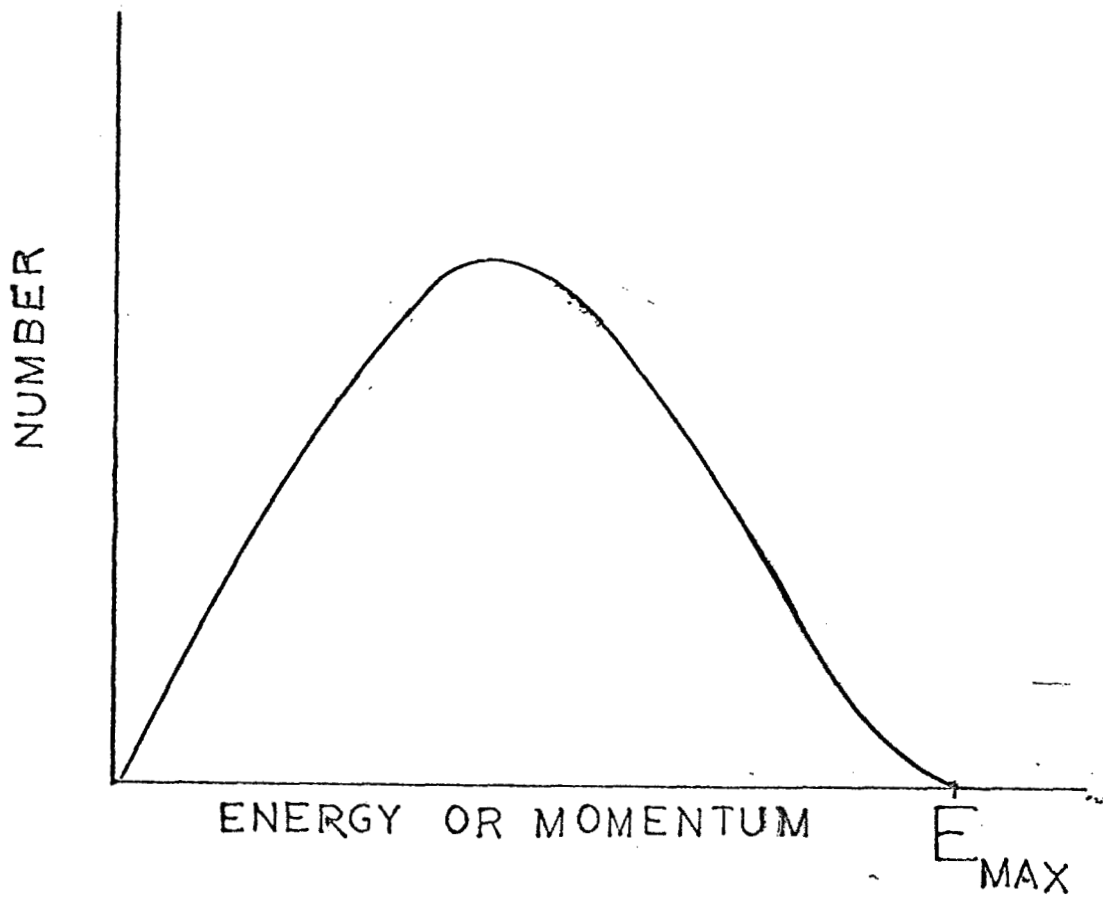
The current produced by the device is due to the emitted β^- particles. These particles are emitted from the source material by the reaction,



A typical energy spectrum for a β^- source is shown in Figure 3 (5, Ch. 17). The kinetic energy of the particle as it leaves the parent nucleus determines the potential which it can overcome on its flight to the collector.

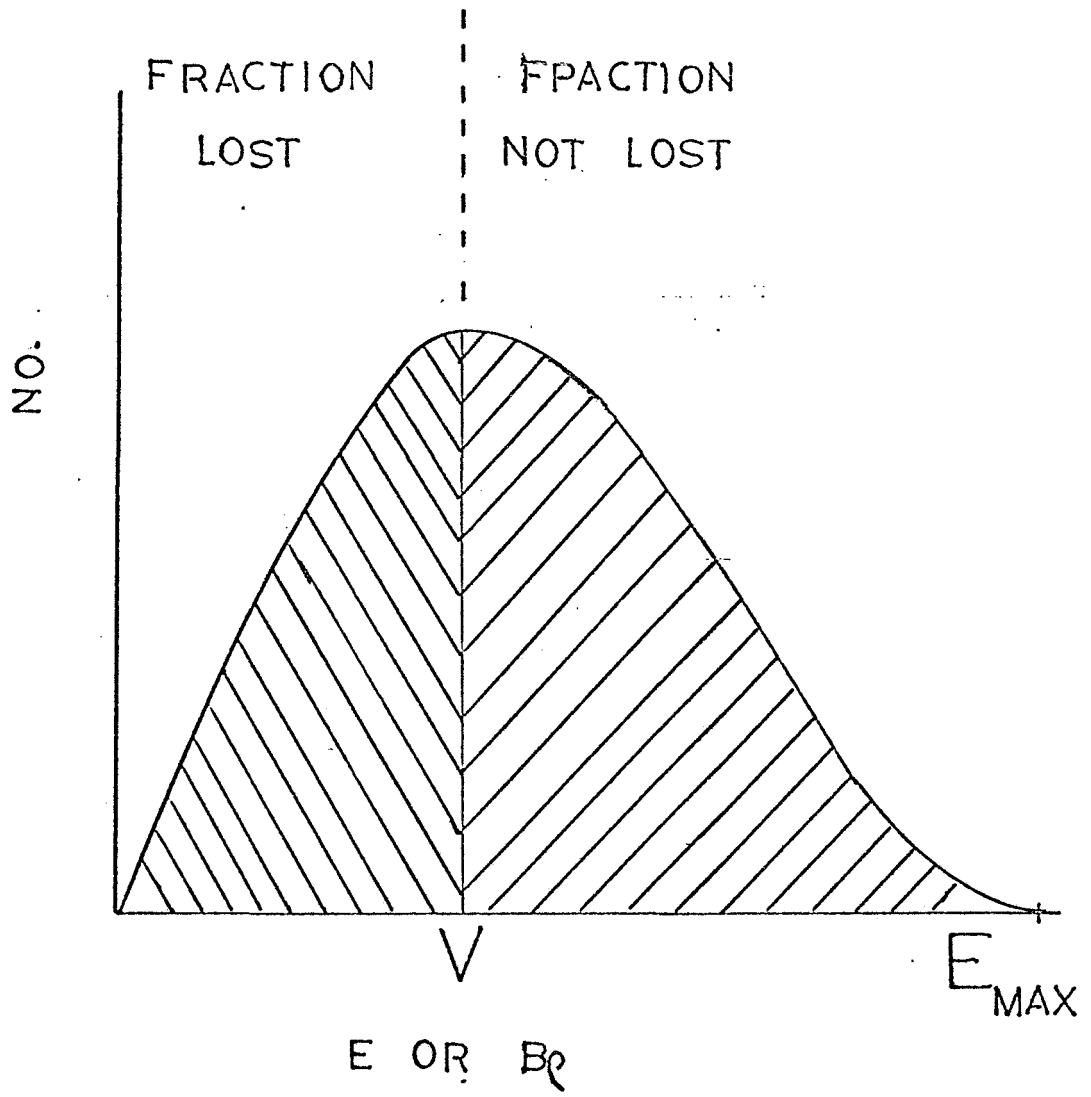
A .3 Mev β^- particle, for example, could overcome a potential of 300 KV if it suffered no collisions during flight. Thus, as shown in Figure 4, the fraction of the area under the curve which lies to the left of potential, V is the fraction of the β^- particles which will not be able to overcome the potential while the fraction of the

FIG-3



TYPICAL β^- SPECTRUM
SHAPE

FIG-4



area to the right of V represents the fraction of the particles which can overcome the potential.

It is evident that if E_{\max} is high enough and V low enough the cutoff energy will lie in the low energy tail of the curve and the current variations with voltage will be small. This is the case with the power source being considered. It should be mentioned that because most particles will not be emitted directly at the collector, only the component of energy directed at the collector will be effective in overcoming the potential. If E_0 is the actual energy of the particle and θ is the angle at which the particle will impact on the collector, the effective energy of the particle is given below.

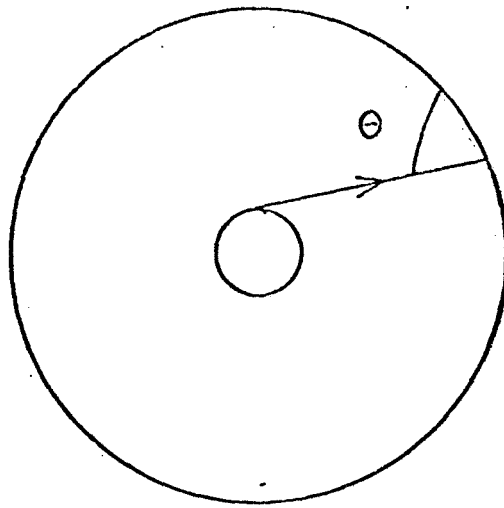
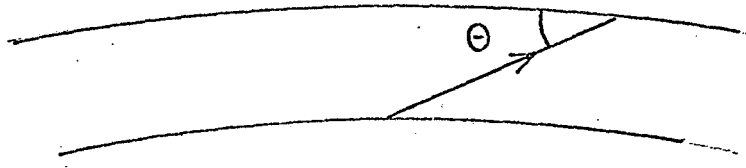
$$E_{\text{eff}} = E_0 \sin \theta.$$

(See Figure 5)

Since E_{eff} is less than E_0 , the fraction of the particles which reaches the collector will be reduced. This effect can be minimized by using a spherical geometry with a small support sphere. As is illustrated in Figure 5, this will make θ close to 90° and, therefore, E_{eff} will be close to E_0 .

The insulating material between the support sphere and the collector must allow passage of the β^- particles with little attenuation or ionization. For a device

FIG-5



operating in space, the obvious insulator would be the vacuum itself. The breakdown voltage of the free space vacuum is considered to be 30 KV/cm for the purpose of this investigation. Thus, a .33 cm separation between the spheres would be required to maintain a 10 KV potential.

At atmospheric pressure, the ionization rate for β^- particles is about 45 ion pairs /cm (5, Ch. 18). At this pressure, the source could not build up a potential because the ions produced in the gas would cancel the accumulating charge. As the gas pressure in the device is reduced, the ionization rate will decrease until in the vacuum of space (10^{-16} - 10^{-17} Torr) the ionization rate will be essentially zero.

The current produced by the source will be the net transfer of β^- particles from the support sphere to the collector. Thus, the losses in the system must be subtracted from the emission rate of the source material. One source of loss, ionization of residual gas in the device, has been discussed and found to be negligible. Other loss mechanisms which must be discussed are self absorption, shadow effects, back scattering and secondary electron production.

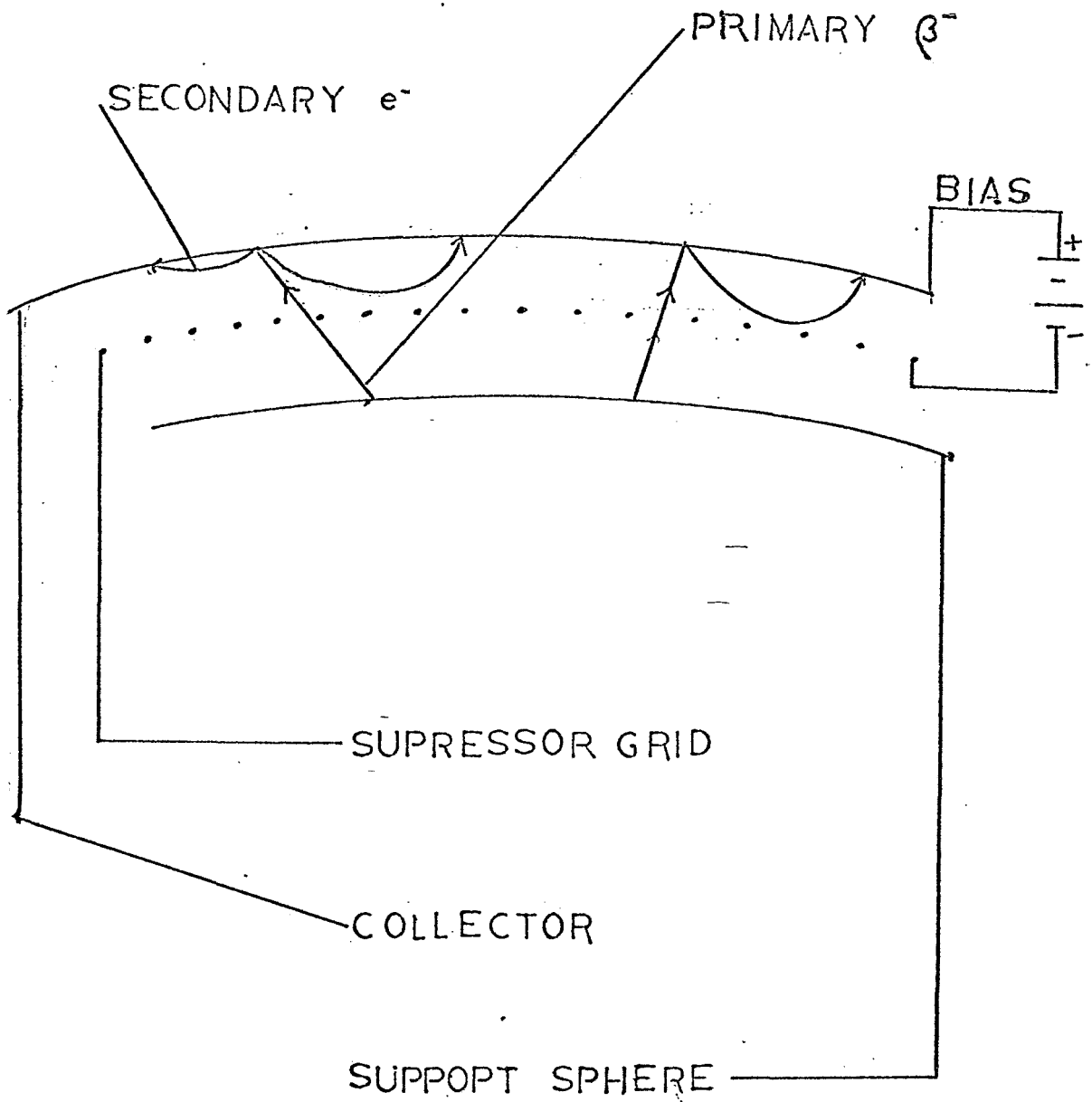
Self absorption as its name suggests is the absorption of β^- particles in the layer of emitting material itself. Shadow effects are similar in that they account for the non-production absorption of β^- particles in the structure

of the power source other than the collector. Back scattering accounts for those particles which may be scattered back out of the collector or out of the support sphere. Secondary electron production accounts for atomic electrons which may be knocked off of the collector by incident β^- particles. Because of the negative charge on the collector, any β^- particle or secondary electron scattered out of it will be accelerated back to the support sphere canceling some of the current.

Two methods of controlling secondary electron emission are available. They are the use of a material with a high work function or the use of a suppressor grid between the two spheres. A material with a high work function will be harder to dislodge electrons from while a suppressor grid charged negatively with respect to the collector would return secondary electrons to the collector as shown in Figure 6. Since no information is available on the production of secondary electrons by high energy β^- spectra, the secondary electron data for this investigation will be experimental.

External radiation dose from the device arises from two sources, the bremsstrahlung from the β^- particles slowing down and any γ rays emitted by the source material. Bremsstrahlung dose may be reduced by using a low Z material in the collector and also by choosing a material which emits only low energy particles. γ dose can be

FIG-6



reduced by choosing a radioactive material which emits very few or very low energy γ rays. These properties of the material must be considered in selecting the best source.

CHAPTER V

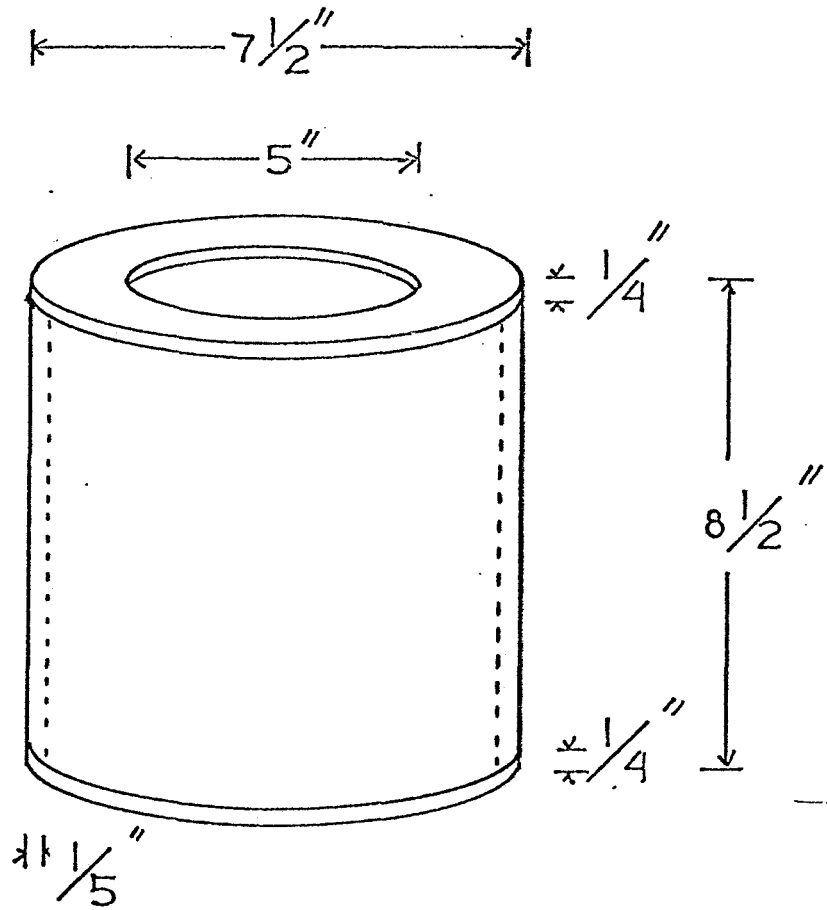
THE EXPERIMENT

The pilot device for the experimental portion of the investigation was constructed of aluminum using P^{32} as a source material. Aluminum was selected because it is easy to machine, has good electrical properties and has a low atomic number to reduce bremsstrahlung. P^{32} was selected because it is a pure β^- emitter which decays to a stable isotope. It is also easily produced in the reactor. The β^- spectrum of P^{32} has an end point energy of 1.7 Mev and has a β^- spectrum similar to Sr^{90} which is expected to be employed in the prototype. The fourteen day half life of P^{32} allows practical observation of the degree to which the current follows the decay of the isotope. Although a spherical geometry is considered most ideal, a cylindrical geometry was used to facilitate fabrication.

Figure 7 shows the details of the collector cylinder. The minimum wall thickness was calculated to be sufficient to stop all of the β^- particles. Various thicknesses were used to save the cost of machining the available stock at the time of construction.

P^{32} for the source was obtained by irradiating Potassium Phosphate Tribasic, $K_3PO_4 \cdot xH_2O$ in the MIT reactor.

FIG 7



COLLECTOR

Prior to irradiation, several samples were dried to determine their weightpercent of water. This value was found to be 12.9%. Care must be taken in determining this number because the material is mildly hygroscopic.

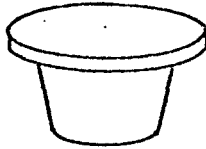
.78722g of $K_3PO_4 \cdot xH_2O$, which contains .100g of natural phosphorous was irradiated in position 23 of the MIT reactor for a period of 4.45 days at a flux level of 5×10^{13} n/cm²-sec. After a five day cooling period, the P³² activity was calculated to be 100 millicuries.

Figure 8 shows the container which held the radioactive material during and after irradiation. It was machined from a standard small irradiation container. The thick section near the top of the cylinder was used to support it while the cap was pressed into place.

Figure 9 shows an exploded view of the central assembly which holds the source container in place. The support rod was machined from a solid aluminum bar, the collar from polyethylene and the bar from lucite. The lucite bar also served as an insulator between the central assembly and the collector. Figure 10 shows the assembled device.

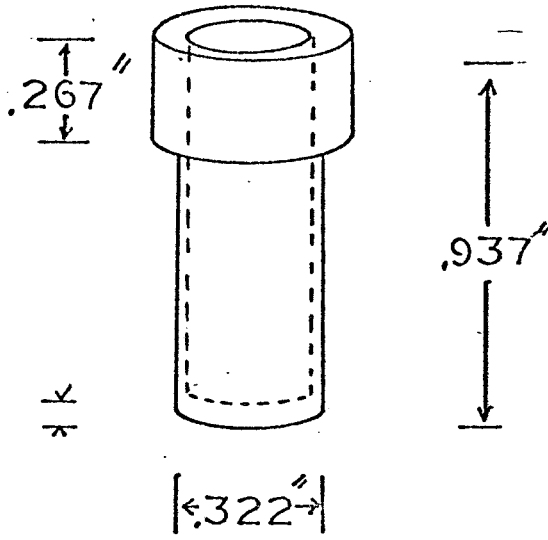
Two vacuum systems were used during the experiment. In the early phases a forepump only system and in the final phase a diffusion pump system. These systems were used to evacuate a bell jar which contained the experimental equipment. In all cases, the vacuum was measured with an error of $\pm 10\%$.

FIG-8



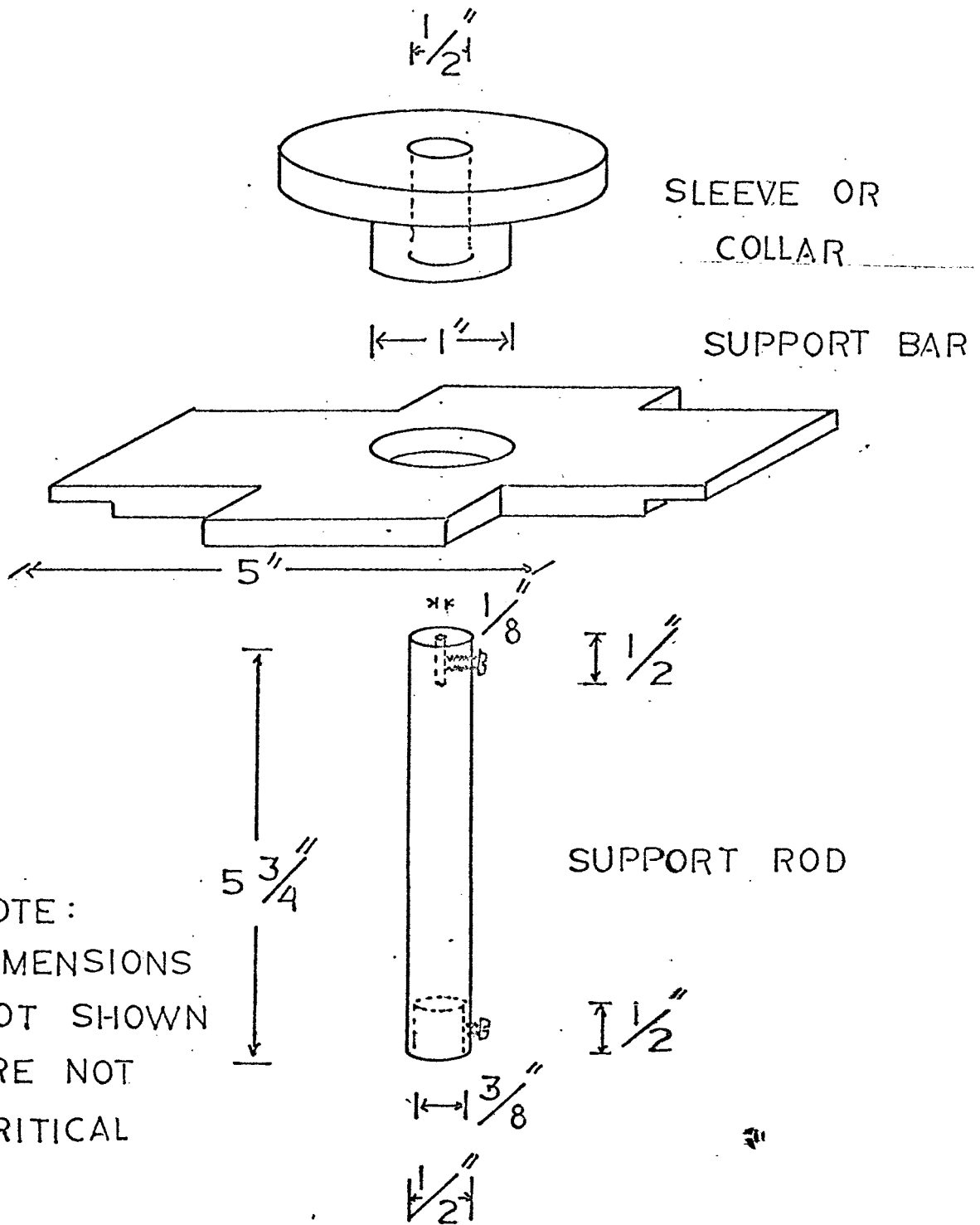
$\left\langle \begin{array}{c} \leftarrow .388 \text{''} \rightarrow \end{array} \right\rangle$

$\lambda \text{ } k \text{ } .031 \text{''}$



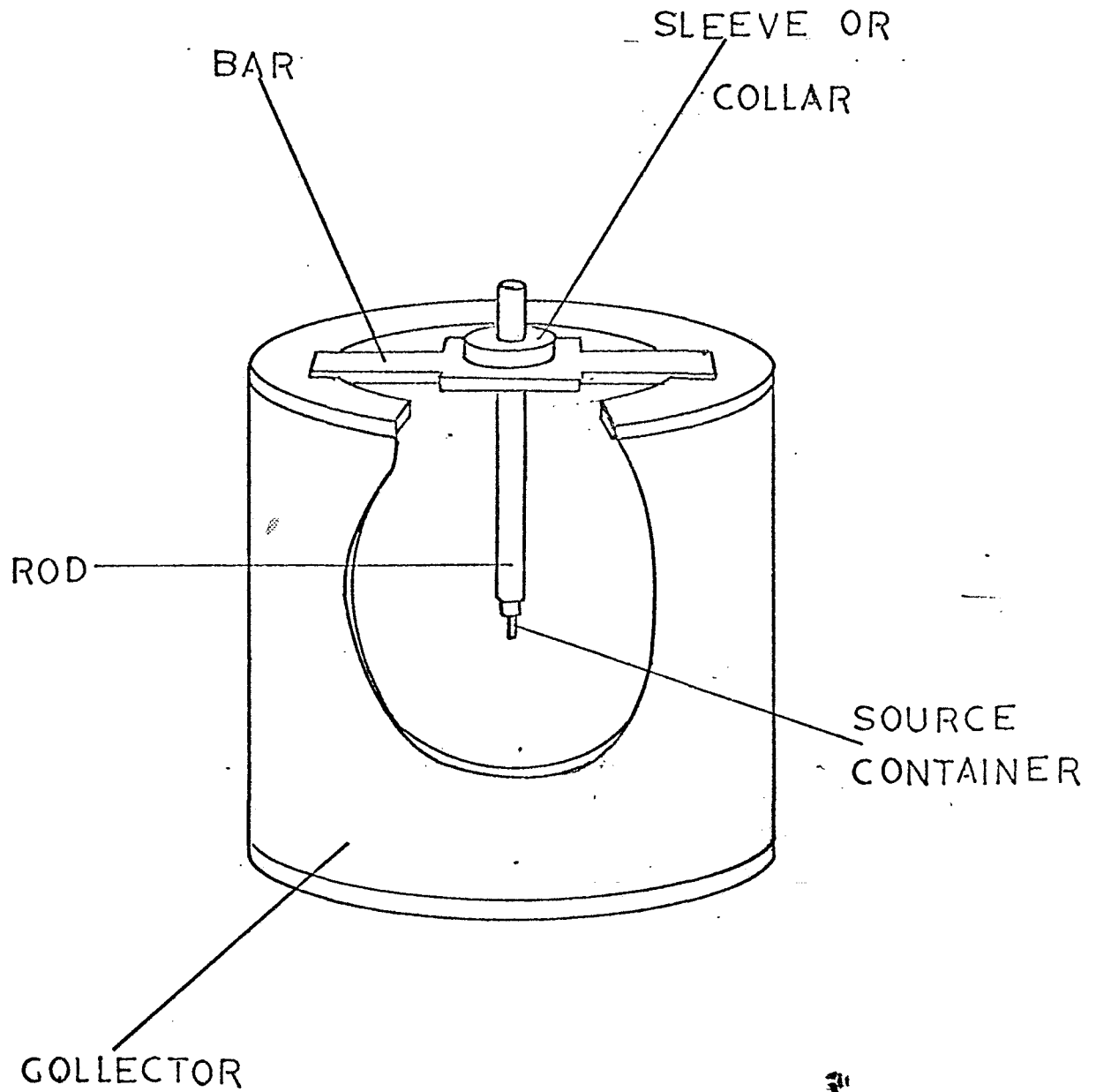
SOURCE CONTAINER

FIG 9



NOTE:
DIMENSIONS
NOT SHOWN
ARE NOT
CRITICAL

FIG-10



Voltage and current measurements which will be described later were made with a Kiethley battery powered electrometer. Model DC VTVM 200 B in the first two phases and a Kiethley Model 610 B Electrometer in the third phase of the experiment. The model 200 B is capable of voltage measurements between .008 and 20 Volts. When used in conjunction with a Decade Current Shunt supplied with the instrument, current measurements between 2×10^{-2} and 8×10^{-14} amps may be made. The model 610 B is capable of voltage measurements from .001 to 100 Volts. It is capable of other measurements but was only used as a voltmeter. The accuracy of both instruments is $\pm 1\%$.

Resistors used in the experiment were manufactured by the Victoreen Instrument Company, Cleveland, Ohio. Eleven resistors in all were used as a load for the device, three ($4 \times 10^{11} \pm 1\%$) Ω resistors and eight ($1.4 \times 10^{11} \pm 10\%$) Ω resistors. All resistors were manufactured under the trade name "Hi Meg".

The capacitor used was an Aerox V146XR-34 paper capacitor with a value of $1\mu\text{f} \pm 10\%$.

The actual experiment was conducted in three phases. In Phase I the current produced by the device was put through a known resistance consisting of the eleven resistors mentioned above connected in series. The purpose of this phase was to determine how well the current put out by the device would follow the decay curve of the P^{32} . From the

known resistance and the measured current, the voltage was also calculated. Due to interference from outside sources, it was found necessary to shield the entire setup with a wire mesh screen.

In Phase II the power source was allowed to charge for a period of time after which it was discharged and the accumulated charge was measured as a voltage on a scaling capacitor according to the relation

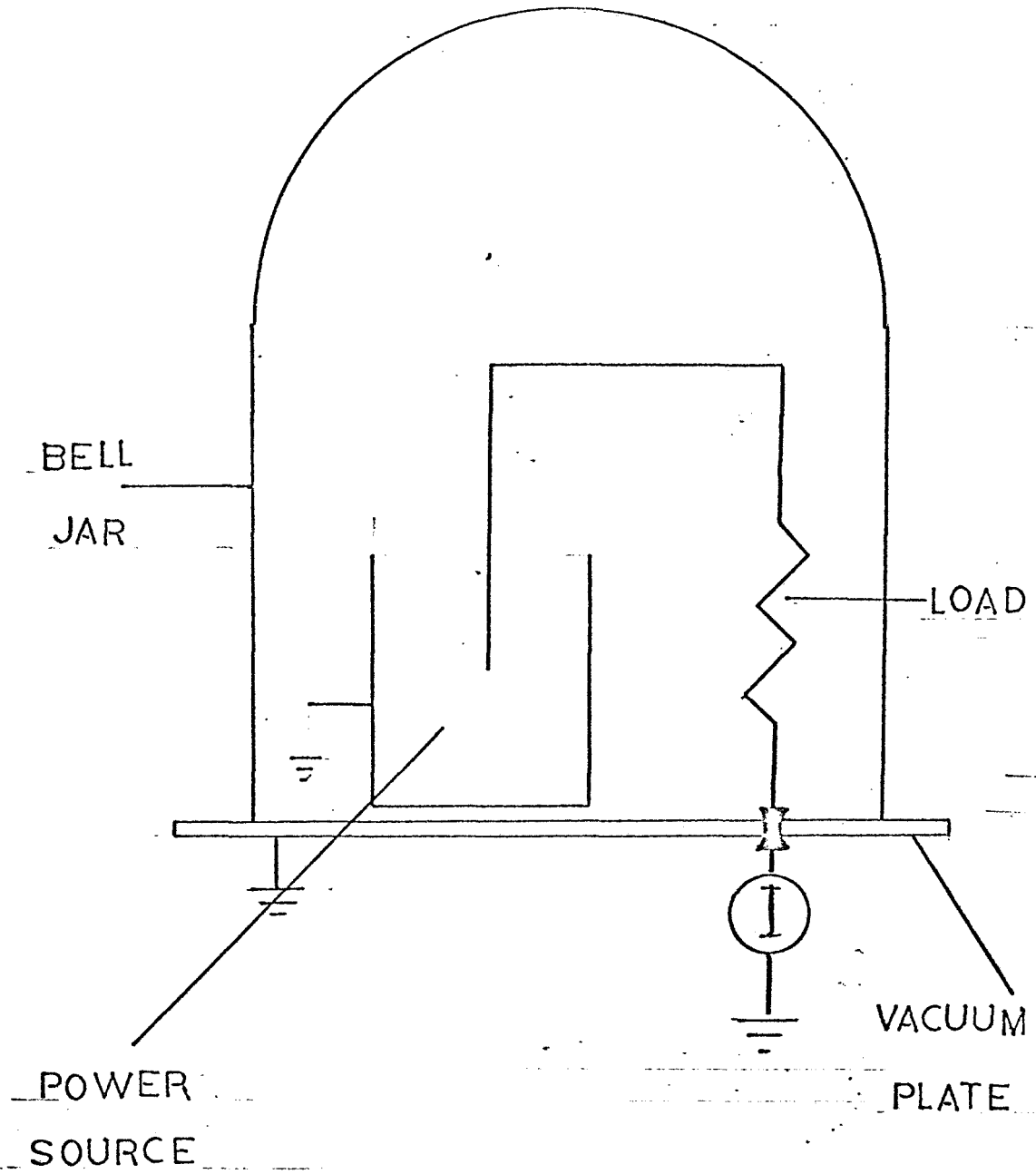
$$V = \frac{vC}{C}$$

where V is the actual voltage on the power source, v is the measured voltage on the scaling capacitor, c is the value of the scaling capacitor and C is the capacitance of the power source. Appendix I contains a derivation of this formula. In Phases I and II, the vacuum system which had only the mechanical pump was used.

Phase III is essentially the same as Phase II, the major difference being that the diffusion pump vacuum system was used instead of the forepump system. The purpose of Phases II and III was to determine the maximum voltage which the device would accommodate.

For all three phases of the experiment, the device was set up as shown in Figure 10. Figure 11 illustrates the wiring scheme for Phase I. The current meter shown was the Model 200 B electrometer set up as a $\mu\mu$ ammeter.

FIG-11



After the system had been evacuated, current measurements were taken over a period of several weeks to establish a decay curve. Figure 12 illustrates the equivalent circuit for Phase I configuration. R_i is the internal resistance of the device and was measured to be about $10^{14}\Omega$. r is the external resistance and was $2.3 \times 10^{12}\Omega$. The measured capacitance of the device was 2.27×10^{-4} farads.

Figure 13 illustrates the wiring for Phases II and III of the experiment. In Phase II, the switching was accomplished by a mousetrap electrically connected to the central assembly. A chain was held away from the trigger by a magnet outside the bell jar. To close the switch, the magnet was removed allowing the falling chain to activate the mousetrap. When the switch was closed the voltage developed on the device was measured on the scaling capacitor reduced by a factor of $\frac{C}{C}$. The voltmeter shown is the 200 B electrometer set up as a voltmeter.

In Phase III the only changes made from Phase II were the substitution of the diffusion pump vacuum system for the forepump system, the 610 B electrometer for the 210 B, and a flat aluminum plate for the mousetrap in the switch. The chain falling on the plate completed the circuit instead of the mousetrap.

FIG-12

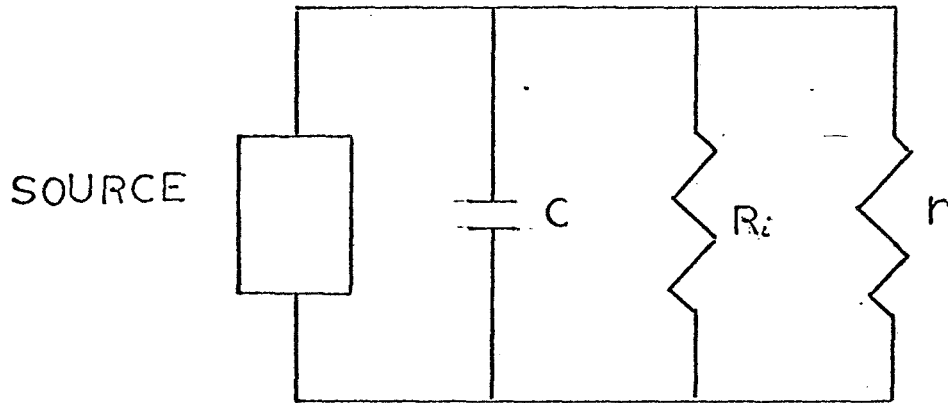
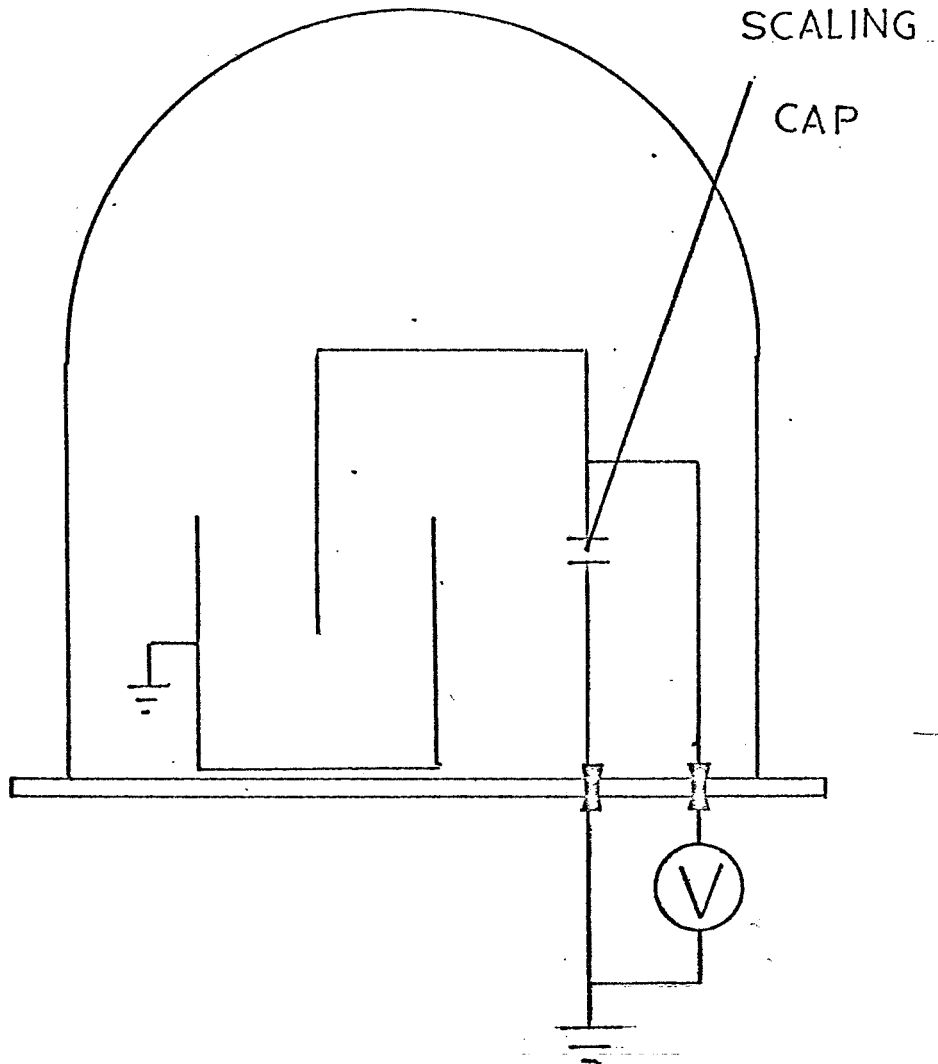


FIG 13



CHAPTER VI
CALCULATIONS AND RESULTS

Table 1 lists the results from phase I. Figure 14 is a plot of the results.

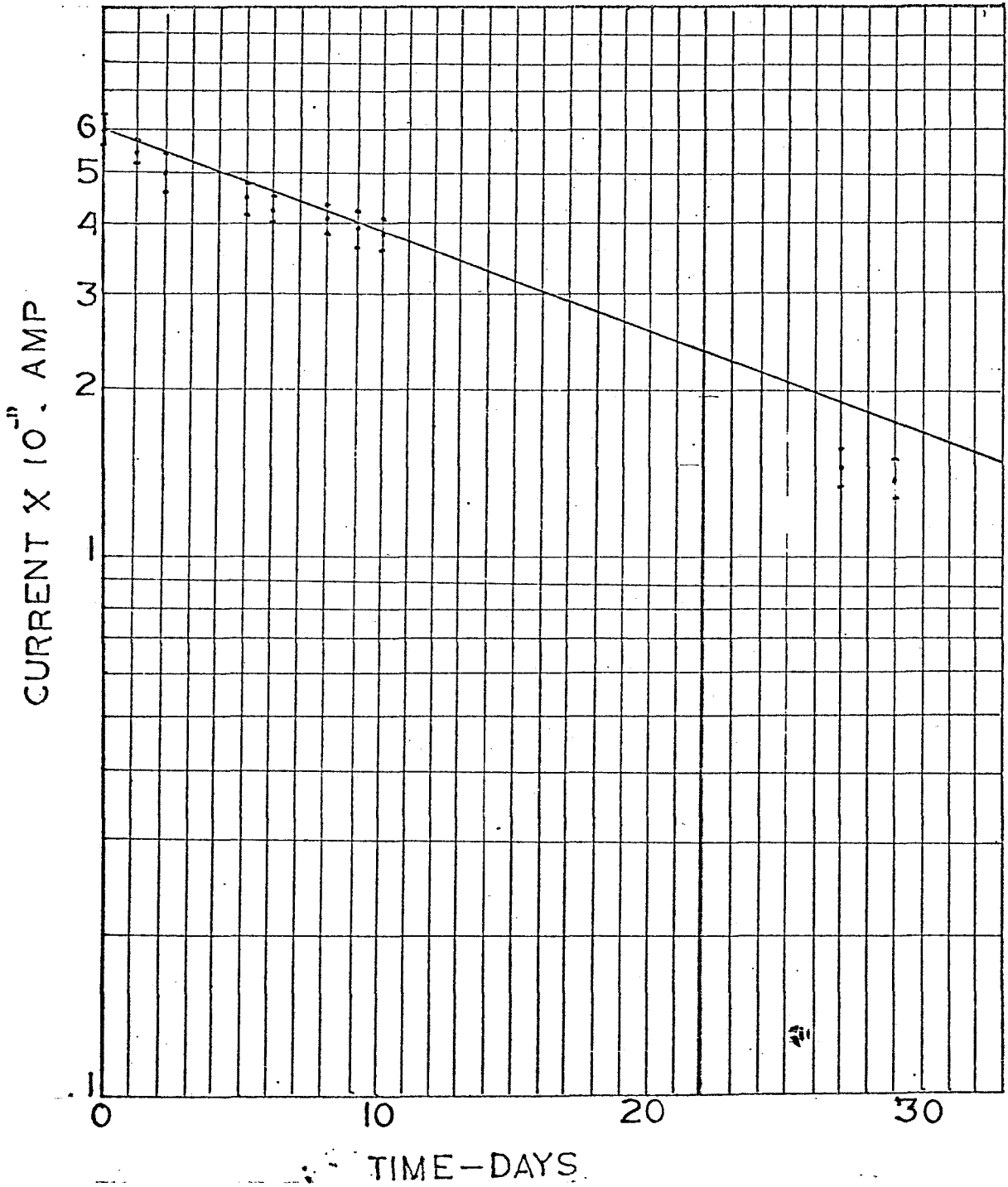
Table 1
Results of Phase I

<u>Date</u>	<u>Vacuum (μ #g)</u>	<u>Current ($\times 10^{-11}$ amps)</u>
14 Jan 1970	40	6.0
15 Jan 1970	22	5.4
16 Jan 1970	21	5.0
18 Jan 1970	18	4.5
20 Jan 1970	19	4.3
21 Jan 1970	17	4.12
22 Jan 1970	17	3.95
23 Jan 1970	18	3.78
10 Feb 1970	40	1.62
12 Feb 1970	31	1.55
20 Feb 1970	40	1.16

A least squares fit of the data shows a half life of 16.4 days. This is within 15% of the 14.3 day half life of P^{32} . It is felt that this value is within acceptable limits due to the interference introduced

FIG-14

CURRENT DECAY



into the current measurements by extraneous electric fields in the vicinity of the instruments.

The total current available from the 100 millicuries of activity was 5.92×10^{-10} amps. Since 6.0×10^{-11} amps was the measured current, only 10.1% of the available β^- particles were being utilized. The measured current would produce 140.5 Volts across the $2.3 \times 10^{12} \Omega$ resistance.

Phase II of the experiment yielded the following results.

Table 2

Phase II Results

<u>Unscaled Voltage</u>	<u>Scale Factor</u>	<u>Act. Voltage</u>	<u>Pressure (mm Hg)</u>
.02 V	4.4×10^4	880 V	1.8×10^{-2}
.009 V	"	496 V	2.5×10^{-2}
.006 V	"	284 V	3.0×10^{-2}
.006 V	"	284 V	3.0×10^{-2}

Phase III yielded the following results.

Table 3

Phase III Results

<u>Unscaled Voltage</u>	<u>Scaled Voltage</u>	<u>Pressure (mm Hg)</u>	<u>Charging Time (Hrs.)</u>
.12	5270 V	2×10^{-5}	7
.141	6200 V	1.9×10^{-5}	28
.155	6820 V	1.9×10^{-5}	24
.152	6680 V	1.9×10^{-5}	25
.151	6640 V	1.9×10^{-5}	69

It should be noted that an upper limit of about 6800 Volts was established.

The accuracy of the measurements in phases II and III is about $\pm 10\%$ due to the uncertainty in the activity of the source and the variations in the circuit components.

CHAPTER VII
INTERPRETATION OF THE RESULTS

It was mentioned before that the actual current put out by the device is the emission rate of the radioactive material less all β^- particles which are lost to the mechanisms mentioned in Chapter III. Each of these loss mechanisms will be applied to the power source treated in the experiment.

Ionization was found to be negligible at the pressures which exist inside the bell jar.

Self absorption in the source material and in the thin wall of the source container was calculated under the assumption that all the β^- particles were emitted from a line source located at the axis of the container, and that an average β^- particle was emitted at an angle of 45° to this line source. Range calculations (5, Ch. 21) showed that 69.6% of the β^- particles emitted from P^{32} did not have the 1.1 Mev required to penetrate the $.517\text{g/cm}^2$ of K_3PO_4 and aluminum which separated them from the surface of the source container if the P^{32} spectrum shape were assumed to be of the same shape as the Sr^{90} spectrum. (See figure 16)

If the source material were approximated by a sphere of the same diameter as the cylindrical source

container, it was found that shadow effects and β^- particles passing through the access hole in the cylinder subtended 20% of the 4π solid angle surrounding the source material. All of these β^- particles were lost to the system.

The thick disk at the bottom of the source container was found to subtend 5.5% of the 4π solid angle around the source, and it attenuated 100% of the β^- particles incident upon it if they first had to penetrate the same thickness of K_3PO_4 as those particles existing through the thin window. Thus, 77.4% of the particles were lost to absorption in one form or another. Since only 10.5% of the available current was measured, 12.1% of the current must have been lost through back scattering and secondary electron production. Back scattering losses at the collector were approximately compensated for by extra electrons knocked off the source container by the β^- particles passing through it. The entire 12.1% discrepancy is, therefore, attributable to secondary electrons produced at the collector. The secondary electron production was, therefore, .536 secondary electrons for each primary β^- particle.

There were two main reasons why Phase II yielded voltages substantially lower than those called for in the problem. These are poor vacuum and the buildup time of the device.

The poor vacuum was the major factor contributing to the low voltage. Figure 15 (10) is a plot of breakdown voltage vs. electrode separation times pressure. Since electrode separation in the pilot device was about 10 cm, it can be seen that the breakdown voltages for the pressures at which Phase II measurements varied from about 400 Volts at 30 microns to about 700 Volts at 18 microns. When the uncertainty of the measured pressure and variations in temperature and humidity are considered, it is felt that the results are near optimum for the pressures used.

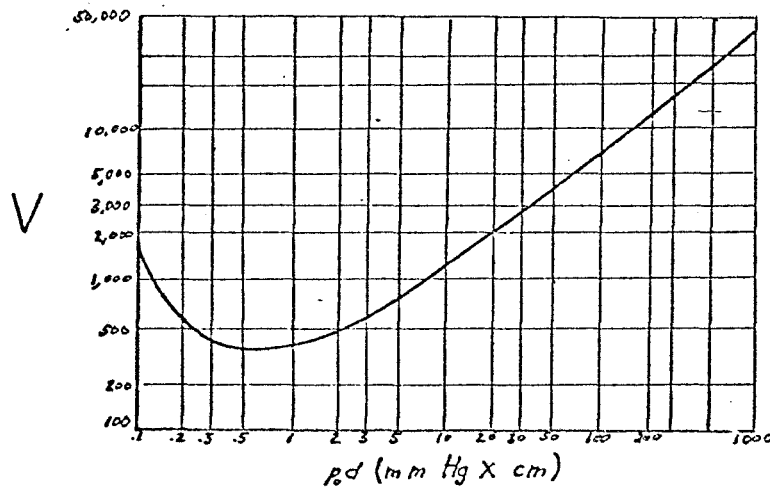
Prior to the closing of the switch, the power source was expected to charge like a simple capacitor according to the equation.

$$\frac{dV}{dt} = \frac{I}{C}$$

At the time Phase II of the experiment was run, the current was about 2×10^{-11} amps. Thus, the charging rate of the device was .85 V/sec. At this rate twenty minutes would be needed for 1000 Volts to build up. Since it was not known when the vacuum became good enough for the device to start charging, it was possible that the voltage was measured at some time prior to the build up of maximum voltage.

The 2×10^{-5} mm Hg vacuum achieved in Phase III allowed higher voltages to be built up. At this pressure,

FIG 15



BREAKDOWN VOLTAGE
IN AIR

the point of operation is far to the left of the minimum pressure in Figure 15. The upper limit in this case is not expected to be due to breakdown but to the fact that charge leakage from irregularities in the structure of the power source at the end point voltage was equal to the rate of charge accumulation from the β^- source. A more carefully constructed device would have attained a higher voltage.

CHAPTER VIII

CONCLUSIONS

From the preceding results it appears that the power source would be a feasible undertaking if it were carefully constructed to minimize losses. Due to its voltage and current characteristics, however, the device would find application only in specialized instrumentation such as charged particle detectors.

The radiation field generated by the device may limit its usefulness near radiation sensitive instruments. The dose may be reduced by either distance or shielding or both, perhaps at the cost of some weight. The radioactive material may require some specialized and, therefore, quite expensive manufacturing and handling techniques. On the other hand, the simple design and lifetime of the power source make it an extremely reliable device for long term applications. It is also thermally insensitive and extremely rugged.

The fact that the upper limit was imposed by the leakage from irregularities in the structure of the device, together with the results obtained by previous investigators, indicates that much higher voltages than 10 KV could be obtained merely by increasing the separation of the two spheres if they were carefully constructed. The current

could be increased by increasing the activity of the source material although this would increase the external dose rate.

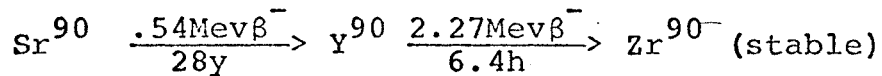
It would appear, nevertheless, that the present level of technology is capable of producing this power source if the need for it were great enough.

CHAPTER IX

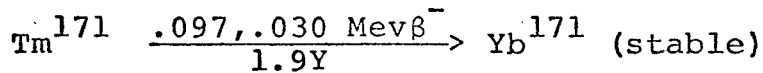
SPECIFIC EXAMPLES

This chapter considers the design of devices using both Sr^{90} and Tm^{171} as a radioactive source material. The design characteristics of the source a μ amp at 10 KV.

Sr^{90} has a 28 year half life and is ideally suited for missions of extreme length. Sr^{90} and its daughter Y^{90} emit high energy β^- particles which give rise to penetrating bremsstrahlung. The reaction is



Tm^{171} , on the other hand, emits very soft β^- particles and a soft γ ray. These emissions give rise to much lower doses than Sr^{90} . The reaction is



The 1.9 year half life of Tm^{171} , however, limits its application to shorter missions on the order of a year in length unless instruments that can tolerate large current ranges are used.

Because less intense bremsstrahlung are generated when β^- particles slow down in low Z materials, the collector and support spheres will be made of beryllium which has a Z of four.

The chemical form of Sr used in the power source will be SrO which is obtainable with a specific activity of 208 curies/cm³. (1) The SrO will be coated on a support as shown in Figure 2.

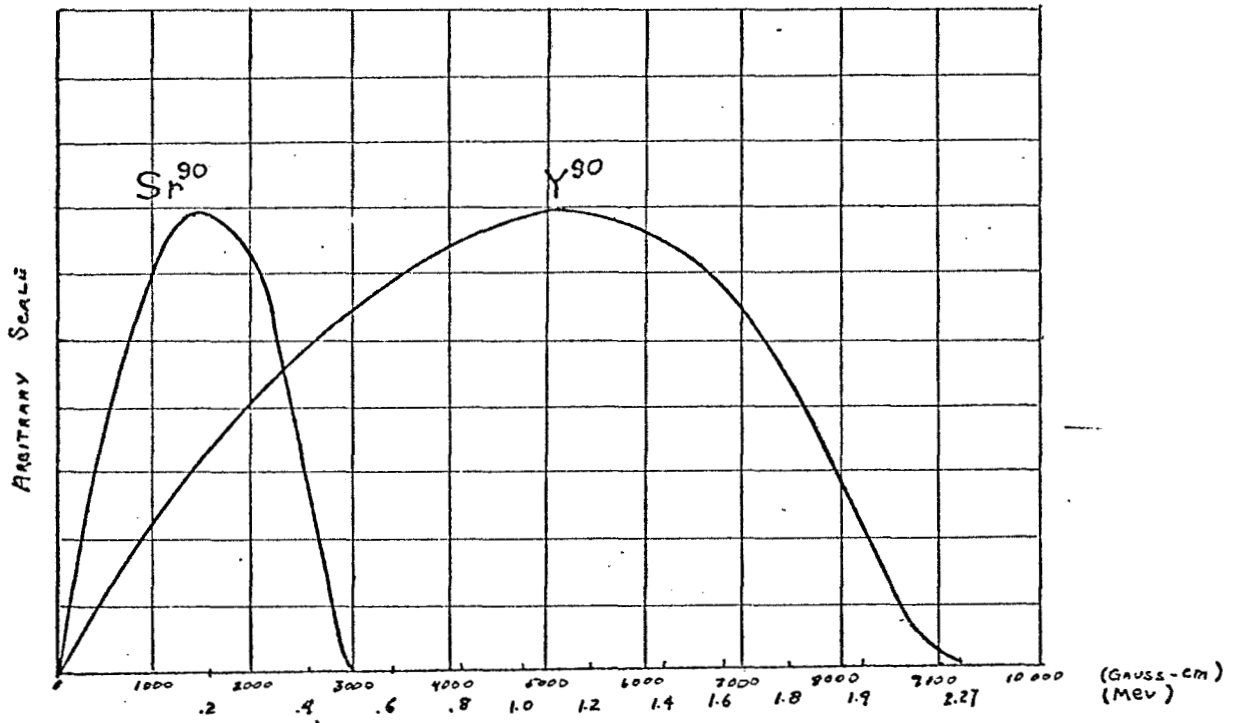
The collector sphere will be thick enough to stop all of the emitted β^- particles. 1400 mg/cm² or .760 cm of beryllium is the range of the 2.27 Mev β^- spectrum from Y⁹⁰ (5, Ch. 21). This then will be the thickness of the collector.

An arbitrary thickness of 1 mm will be used for the support sphere.

The amount of activity deposited on the support sphere must be sufficient to supply the 1 μ amp of current required. Figure 16 shows that at 10 KV essentially all the particles emitted from the source will reach the collector. No losses due to potential will be considered.

1 μ amp is equivalent to 6.24×10^{12} β^- particles per second or 168 curies at 100% collection efficiency. Since the decay scheme of Sr⁹⁰ yields two particles for each decay only 84 curies would be required at 100% collection efficiency. If the source is designed to give 1 μ amp at a point halfway through a five year mission, the decay of the isotope will require 91.5 curies at the beginning of

FIG-16



Sr⁹⁰ - Y⁹⁰ β⁻ SPECTRA

the mission. Half of the particles emitted from the source material will enter the support sphere. If it is assumed that the range required for such a particle to completely penetrate the sphere and emerge on the other side is 3 mm of beryllium or $.555 \text{ g/cm}^2$, it can be shown that only 41.4% of the Y^{90} spectrum will penetrate the sphere. Thus, 21.2% of the emission rate into the sphere and 10.6% of the total emission rate in all directions will penetrate the support sphere. This fact will boost the minimum activity to 151 curies.

Some of the β^- particles which enter the support sphere will be scattered back out. This effect may be calculated from the back scattering cross section

$$T_b = \frac{1}{4} \frac{Z^2}{\beta^4}$$

where $\beta = \frac{v}{c}$ (5, Ch. 20)

Because back scattering accounts for less than 6% of the total β^- particle population and because back scattering will occur at both the support sphere and the collector, it is assumed that the effect cancels itself out.

The only remaining loss mechanisms to be considered are the production of secondary electrons and self absorption. If the assumption is made that the secondary electron production ratio is the same for beryllium as for aluminum, the total amount of activity required will be

326 curies. This amount of activity contained in SrO will weigh 5.80 g and would be a layer .0050 cm or .0184 g/cm² thick on a support sphere of 5 cm radius. The energy of a β^- particle with this range is .1 Mev. The fraction of the combined Sr⁹⁰, Y⁹⁰ spectrum which lies below this energy is about 9%. (See Figure 16) Therefore, the final amount of activity required for the source to produce 1 μ amp will be 350 curies.

The external dose level from this power source will be due to bremsstrahlung. The dose level may be calculated from the fact that the bremsstrahlung intensity from a given source is directly proportional to the Z of the material in which the β^- particles slow down. (5, Ch. 21) It can be shown from Arnold (1) that the dose from a beryllium power source using Sr⁹⁰ as a radioactive material will be 454 mr/hr at one meter.

If 12KV is the design voltage of the power source to allow a safety factor in the 10 KV rating, the sphere separation will be .4 cm and the device will weigh 650 g or 1.43 lbs.

The dose may be reduced by methods stated in an earlier chapter. Because they are generated by high energy β^- particles, the bremsstrahlung will be very difficult to shield against. A device of the size above shielded with one centimeter of lead will weight over 10 lbs. and the dose will be reduced only by a factor of 2. (5, Ch. 25)

Tm^{171} may be substituted for the Sr^{90} as a β^- emitter.

Tm^{171} may be obtained in the chemical form Tm_2O_3 with a specific activity of 8648 ci/cm^3 . (1) The emissions are predominantly $.097 \text{ Mev } \beta^-$ particles and a $.067 \text{ Mev } \gamma$ ray. In 2% of the decays a $.03 \text{ Mev } \beta^-$ particle is emitted, but these are ignored in this chapter.

Because the range of the β^- particle is only $.013 \text{ g/cm}^2$ or $.007 \text{ cm}$ of beryllium the collector need be only thick enough to be structurally sound. The activity required to produce 1μ amp of current may be calculated to be 743 curies exclusive of self absorption effects. The two main considerations which are different in this case from the Sr^{90} source are the particles emitted into the sphere are absorbed completely instead of a few penetrating, and allowance must be made for the fact that an appreciable fraction of the β^- spectrum will not overcome the 10 KV potential applied to the source.

The short range of the emitted particles requires that a very thin layer of Tm_2O_3 be deposited on the surface of the support sphere. If a thick layer were present only a thin layer of material would be contributing to the current produced by the device.

If a 15 cm radius were used for the support sphere, a total of about 1500 curies would be required to produce.

1 μ amp after self absorption was considered. Assuming a .4 cm sphere separation and a 1 mm thickness for both spheres, the weight of the device would be 2.58 lbs.

The external dose rate may be calculated to be 24.7 mr/hr at one meter. (1) This dose is very much lower than that for a Sr⁹⁰ source. It is a much softer dose as well. The equivalent of one centimeter of lead will reduce the dose by a factor of 2.5×10^{-3} .

The major drawback to the use of Tm¹⁷¹ is, as has been stated earlier, its short half life.

Although spherical geometry was considered above, construction difficulties may warrant the use of a cylindrical geometry. This would introduce some extra weight and some current losses due to edge effects. The saving in manufacturing cost may justify these losses.

APPENDIX I

DERIVATION OF THE VOLTAGE SCALING RELATIONSHIP

The experimental setup for Phase II may be viewed as shown in Figure 17. Figure 17A is the device prior to the closing of the switch. C_1 and C_2 are the capacitance values of the scaling capacitor and the power source respectively. q_1 and q_2 represent charge on each capacitor and V_1 and V_2 are the voltages on the two capacitors. Figure 17B shows the device after the switch has been closed. The primed letters represent the same quantities as above after the switch has been closed.

Before the switch is closed,

$$V_1 = q_1 = 0$$

V_2 is the charge built up on the power source by the accumulated charge q_2 .

$$1) \quad C_2 = \frac{q_2}{V_2}$$

After the switch is closed,

$$2) \quad q_1' + q_2' = q_2$$

$$3) \quad C_1 = \frac{q_1'}{V_1'}$$

$$4) \quad C_2 = \frac{q_2'}{V_2'}$$

$$5) \quad V_1' = V_2'$$

From equations 1) and 2),

$$C_2 = \frac{q_1' + q_2'}{V_2}$$

From equations 3) and 4),

$$C_2 = \frac{C_1 V_1' + C_2 V_2'}{V_2}$$

From equation 5),

$$C_2 = \frac{C_1 V_1' + C_2 V_1'}{V_2}$$

But, $C_1 = 1 \times 10^{-6}$ f and $C_2 = 2.27 \times 10^{-11}$ f.

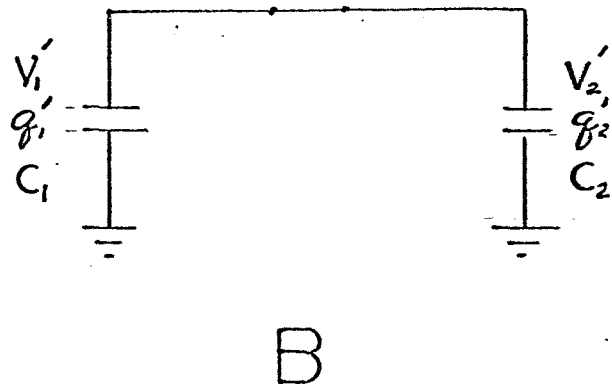
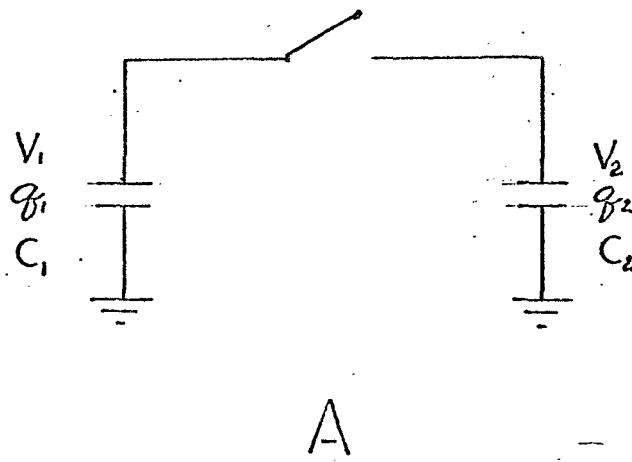
Therefore,

$$C_2 \approx \frac{C_1 V_1'}{V_2}$$

$$V_2 \approx \frac{C_1}{C_2} V_1'$$

Or the actual voltage on the device is very close to the voltage measured on the scaling capacitor multiplied by the ratio of the capacitance of the scaling capacitor to the capacitance of the power source itself.

FIG-17



REFERENCES

1. Arnold, E.D., "Handbook of Shielding Requirements and Radiation Characteristics of Isotopic Power Sources for Terrestrial, Marine, and Space Applications," ORNL - 3576. United States Atomic Energy Commission, Division of Technical Information, 1964.
2. Coleman, J.H., "Radio Isotopic High Potential, Low Current Sources," Nucleonics, 11 (December 1953), 42.
3. Corliss, W.R. and D.G. Harvey, Radio-Isotopic Power Generation, Prentice-Hall, Inc., Englewood Cliffs, N.J., 1964.
4. Diekamp, H.M., Nuclear Space Power Systems, Atomics International, Canoga Park, California, 1967.
5. Evans, R.D., The Atomic Nucleus, McGraw-Hill, New York, 1967.
6. Langer, L.M. and H.C. Price, Jr., "Beta Spectra of Forbidden Transitions," Physical Review, 76 (1949) 641.
7. Linde, E.G., "Nuclear Electrostatic Generator," Physical Review, 71 (1947) 129.
8. Linde, E.G. and S.M. Christian, "The Use of Radioactive Material for the Generation of High Voltages," Physical Review, 83 (1951) 233.
9. Linder, E.G. and S.M. Christian, "The Use of Radioactive Material for the Generation of High Voltages," Journal of Applied Physics, 23 (November 1952) 1213.
10. Meek, J.M. and J.D. Craggs, Electrical Breakdown of Gases, The Clarendon Press, Oxford, 1953.
11. Moseley, H.G.J., "The Attainment of High Potentials by the Use of Radium," Proceedings of the Royal Society of London, 88 (1913) 471.